

Synthesis and Photocatalytic Activity of Nanosized Powder of Zn-Doped Titanium Dioxide

E. M. Bayan^{a,*}, T. G. Lupeiko^a, and L. E. Pustovaya^b

^aSouth Federal University, Rostov-on-Don, Russia

^bDon State Technical University, Rostov-on-Don, Russia

*e-mail: ekbayan@sfnedu.ru

Received December 27, 2017

Abstract—Nanosized powder materials made Zn-doped titanium dioxide with concentration of 0.1, 0.5, and 1.0 mol % Zn²⁺ have been synthesized from aqueous solutions of inorganic compounds of titanium modified with zinc(II) ions. The materials obtained have been studied by electron microscopy, thermogravimetric analysis, and powder X-ray diffraction. It has been found that if zinc ions introduced in titanium dioxide the stabilization of anatase modification takes place retaining size and morphology of particles. The materials synthesized have shown photocatalytic activity under ultraviolet and visible light irradiation. The highest photocatalytic activity has been found for material containing 0.1 mol % Zn²⁺ and calcined at 600°C.

Keywords: nanomaterials, nanoparticles, titanium dioxide, photocatalytic activity

DOI: 10.1134/S1990793118050159

INTRODUCTION

At the present time, semiconducting nanosized materials based on titanium dioxide (TiO₂) are actively used in different regions owing to their unique physicochemical and optical properties, low cost, chemical stability, and toxic safety [1–4]. Photocatalytic properties have a specific interest because of the possibility their applications for purification of aqueous [5, 6] and air media from different organic contaminations using sunlight [7–10]. However, pure titanium dioxide has relatively broad forbidden zone of 3.2 eV [11, 12] and a high rate of recombination of photosensitized supports; this decreases the efficiency of photocatalysis and significantly limits its possibility [13, 14]. To improve their photocatalytic activity (PCA) and to shift the adsorption edge to visible region, titanium dioxide is successfully doped with nonmetals [15–18] and metal ions [19–23] or their combination [24, 25]. Cations of different metals are capable of broadening the absorption spectrum of titanium dioxide and enhance the efficiency of PCA owing to decreases in the degree of recombination of electron-hole pairs generated in the photocatalytic process.

To obtain powders based on TiO₂ modified with Zn(II), sol–gel methods were proposed using stearic acid and titanium-organic precursors [26, 27], as well as hydrothermal-ultrasonic synthesis and other methods [25–28]. This shows that the method of synthesis influences the morphology, size, and crystallinity of material particles, as well as the nature and concentration of the impurities both change the distribution of

charge on its surface, and this significantly influences the PCA of titanium dioxide [25]. In particular, it was found that alloying titanium dioxide with 0.1 mol % of Zn(II) makes greater PCA possible than with a catalyst created via industrial production through Degussa P25 [26]. Therefore, additional study of alloying with zinc is becoming more and more interesting. It is rather difficult at present to predict at which phase ratio the composites of ZnO–TiO₂ composition will show maximum photocatalytic efficiency because this depends on many factors, such as the method and conditions of synthesis and the size and structure of the materials obtained. In this connection, it is necessary to conduct additional investigations to identify the materials synthesized using the new method. In this connection, the results are here given resulting from an investigation of properties of materials based on titanium dioxide obtained using the method of low-temperature cooling and modified with zinc ions from 0.1 to 1.0 mol %.

EXPERIMENTAL

Titanium tetrachloride TiCl₄ (chemically pure grade), zinc sulfate crystalline hydrate ZnSO₄ · 7H₂O (chemically pure grade), 25% ammonia solution (chemically pure grade), and distilled water and oxides of titanium and zinc were obtained using coprecipitation of Ti(IV) and Zn(II) hydroxides from the corresponding solution with given concentrations of salts and their subsequent drying and calcination. The con-

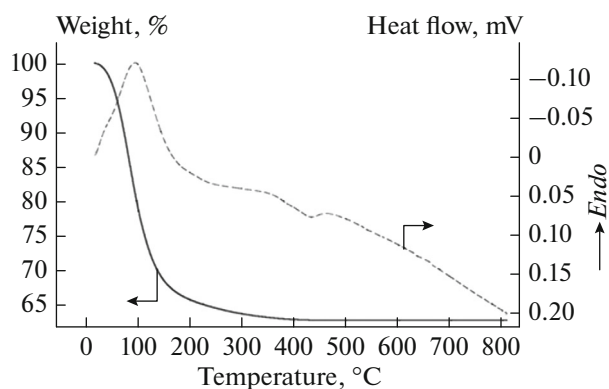


Fig. 1. The data of derivatographic and thermogravimetric analyses of TiO_2 -0.1 mol % of Zn^{2+} .

ditions of synthesis were selected based on previously conducted investigations [29–32]. Coprecipitation was carried out from an ammonia solution from aqueous solutions of titanium chloride of given concentrations prepared from titanium tetrachloride and zinc sulfate within a temperature range from 0 to 5°C and a final pH value from 7.0–7.5. To remove impurity ions, the precipitate obtained was rinsed using distilled water until a negative reaction of the rinsing solutions onto the chloride-ions was attained. The completeness of the deposition of Zn(II) ions in the precipitate was controlled using the photometric method according to the conventions of the use of dithizone.

The precipitates obtained were separated from the solution, dried at 80°C and thermally treated at 500 or 600°C using isothermal exposure for 2 h. Titanium dioxide materials containing 0.1 (0.1% Zn-TiO_2), 0.5 (0.5% Zn-TiO_2) and 1.0 mol % Zn^{2+} (1% Zn-TiO_2) were prepared.

METHOD OF INVESTIGATION

The phase composition of the samples obtained was studied using the X-ray diffractometer Arl X'tra, manufactured by ThermoFisher (Switzerland), using $\text{Cu}(K_{\alpha 1})$ radiation in the range from 20 to 60°C. To evaluate the average particle size, the materials synthesized were recorded in the mixture with large crystal aluminum oxide as a standard. Then, the regions of coherent scattered from the broadening lines of the X-ray, according to Debye–Scherrer equation [33]:

$$d = \frac{k\lambda}{\beta \cos \theta},$$

where $\lambda = 0.1540562$ nm is the wave length of the X-ray radiation, k is the factor for the particle form (it is assumed for spherical particles that $k = 0.94$), β is the line width at half weight of maximal diffraction peak (101) for anatase, and θ is the diffraction angle.

To study the thermal processes, a thermogravimetric and differential–thermal analysis method was used with the heat analyzer TG–DTA/DSC STA 449°S/4G Jupiter Jupted. The samples were heated in air from 298 to 1000 K, using a rate of 10 grad/min. The morphologic characteristics of the material were determined using method of transparent electron microscopy (TEM) using a microscope TEM Tecnai G2 Spirit Bio TWIN.

The PCA of the samples obtained was studied on the model reaction of photodegradation of organic cationic type dyestuff of methylene blue (MB) in titanium dioxide aqueous suspensions under conditions of visible light irradiation (a day light lamp with a power of 40 W with a color temperature of 6400 K) under the action of UV radiation (mercury lamp of low pressure of 10 W power, where the maximal intensity range of UV radiation is 240–270 nm). The qualitative PCA of the phase obtained was evaluated through the degradation of MB to find its the residual concentration spectrophotometrically (using the spectrophotometer UNIKO 1201, $\lambda = 670$ nm, $l = 10$ mm). Every run was repeated not less than three times.

RESULTS AND DISCUSSION

In coprecipitation, Ti^{4+} and Zn^{2+} ions were practically completely transferred into the precipitate, and this was confirmed by quantitative chemical analysis. The precipitates were obtained by X-ray.

To select optimal temperatures of thermal treatment of materials, thermal and thermogravimetric analyses of synthesized samples were carried out. In Fig. 1, for example, a derivatogram of the sample of titanium dioxide is given, doped with 0.1 mol % of zinc. Within the temperature range 80–100°C, an endothermic peak was observed, and an intense decrease in mass takes place, mainly owing to the removal of absorption water. Further decreases in mass took place until temperature of 400°C was attained due to decomposition of titanium(IV) oxohydroxocompounds and zinc(II), and then the substance mass was stabilized. Within the temperature range from 400 to 800°C, against the background of a constant sample mass, a small exothermic peak at 440°C was observed, which is connected with the formation of anatase crystal phase and this is confirmed with X-ray phase analysis (Fig. 2). No pronounced thermal effects were observed, i.e., the substance formed is one-phase and thermally stable to 800°C, unlike what was found in [34], where the materials were described with higher contents of the modified additive: from 0.1 to 0.35 mol % ZnO/TiO_2 . The total mass loss due to water evaporation was about 38.4%; therefore, the composition of the initial phase can be described by the formula $\text{TiO}_2 \cdot 2\text{H}_2\text{O}$. Note that derivatograms of pure titanium dioxide [35] and modified with 0.1 mol % of Zn^{2+} have the same appearance,

and this can be explained with small amount of the introduced additive.

Data from thermogravimetric analyses allow us to select the following temperature modes for the further thermal treatment of materials: 500, 600, 700, and 800°C. X-ray patterns of the materials studied based on titanium dioxide modified with Zn^{2+} in the amount of 0.1 mol % in thermal treatment indicated that they are X-ray amorphous. After thermal treatment to 800°C, the materials had an anatase crystal phase (Fig. 2). The content of anatase crystal modification increased with the temperature of thermal treatment. Peaks of rutile and brookite were absent in the X-ray pattern.

The X-ray pattern in Fig. 2 shows that if the temperature increases to 800°C, the catalytic active anatase modification of titanium dioxide is stable. For pure titanium dioxide, depending on the method of production, the transition of anatase to rutile occurs at 600–700°C [30, 36]. When some metal cations introduce (iron [35, 37], cobalt, nickel [38] and others [39]), the transition of anatase to rutile takes place at lower temperature. Therefore, one can conclude that the introduction of Zn^{2+} in the amount of 0.1–1% stabilizes the anatase modification. These conclusions support the results of previous investigations [34, 40, 41]. Increases in the temperature of thermal treatment leads to increase of intensity and decrease in peak width in X-ray patterns, indicating material crystallization.

Based on the positions of anatase (101) peaks in X-ray patterns, the average size of crystallites was found to be 12–25 nm (Table 1). Increases in the temperature of thermal treatment led to small increases in particle size and were, evidently, connected with the crystallization of titanium dioxide and accompanying agglomeration. It can also be concluded that particle sizes changed slightly with both temperature and amounts of zinc ions in the samples.

With increases in thermal treatment, the processes of crystallization proceeded more actively. This led to increases in particle size and decreases in the specific surface of final powder materials.

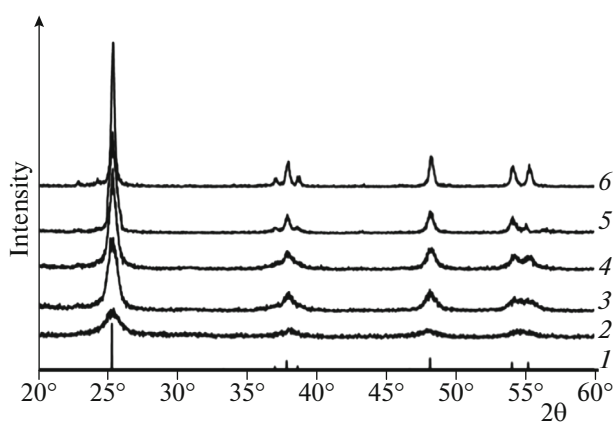


Fig. 2. X-ray pattern of materials doped with Zn^{2+} ions in amount of 0.1 mol %, held at 120°C (curve 2), 500°C (curve 3), 600°C (curve 4), 700°C (curve 5) and 800°C (curve 6), as well the X-ray pattern of the sample of its anatase modification from the data base PDF-2 (curve 1).

Based on the TEM study (Fig. 3), particles of synthesized nanomaterials tended to aggregate to form conglomerates of several hundred nanometers in size, and this could decrease their catalytic activity. The individual particles of these conglomerates have dimensions of ~10–20 nm, depending on preparation conditions, as well as well-defined boundaries and a nearly spherical shape, factors that make it possible to use the Debye–Scherrer equation to determine their size from the broadening of the X-ray reflexes. Note also that the Zn^{2+} -doped samples are agglomerated less than pure titanium dioxide obtained by the same method [30].

The results of PCA investigations of the samples obtained are given graphically (Fig. 4) as the dependence of fractions of photodegraded MB on contact time with a catalyst. As seen from Fig. 4, all synthesized nanomaterials doped with zinc(II) ions and calcined at 500 and 600°C had PCA in the UV spectral region. The PCA of samples after thermal treatment at 500°C were practically the same, and after burning at 600°C, the PCA was markedly higher than the corre-

Table 1. Conditions of synthesis and properties of titanium dioxide nanomaterials doped with zinc

Thermal treatment temperature, °C	Particle size*, nm			
	TiO ₂	0.1% Zn–TiO ₂	0.5% Zn–TiO ₂	1% Zn–TiO ₂
500	9	12	14	14
600	13	15	18	19
700	18	21	21	23
800	21	23	23	24

* Particle size was evaluated from the regions of coherent scattering calculated from X-ray phase analysis data.

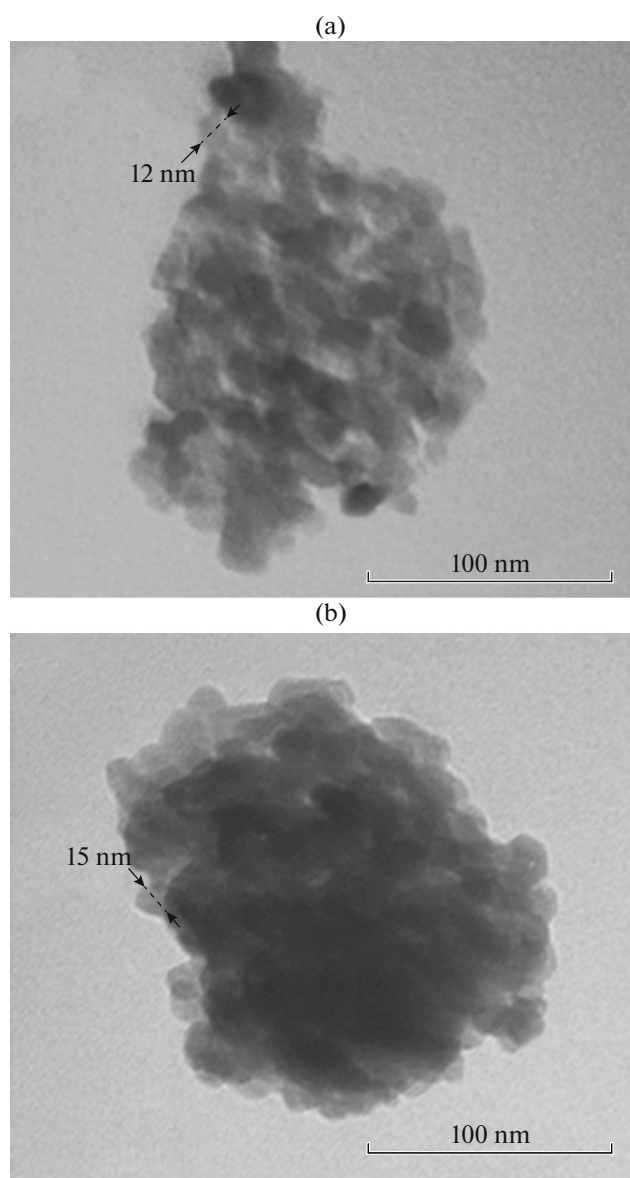


Fig. 3. TEM patterns of dioxide titanium sample modified with 1 mol % of Zn^{2+} , and calcined at (a) 500°C and (b) 600°C .

sponding catalyst activity based on titanium dioxide Degussa P25 from industrial production.

The samples studied showed high PCA under the action of not only ultraviolet radiation but also visible light (Fig. 5). As was shown in examination [23] through absorption-UV spectroscopy, doping with Zn^{2+} decreases the width of the forbidden zone (to 2.7 eV) and makes it possible for modified material to show the PCA in the visible spectral part.

Materials calcined at 600°C (Figs. 4b, 5b) showed higher PCA compared with nanomaterials subjected to burning at 500°C (Figs. 4a, 5a). Also note that the

samples studied reproduced the rate of photocatalytic degradation, even after five repeated cycles.

According to the theory of heterogeneous catalysis, the amount of active centers on the surface of material is factors influencing the rate of reaction; these centers actively form when there are defects on the surface [35]. The introduction of small number of modified additives led to a distortion of the crystal lattice and a violation of electrical neutrality, and this was the reason for the increase in the PCA. The effect appeared for nanosized particles with a high specific surface. When doped values are determined, it is necessary to consider that the introduction of a material that is

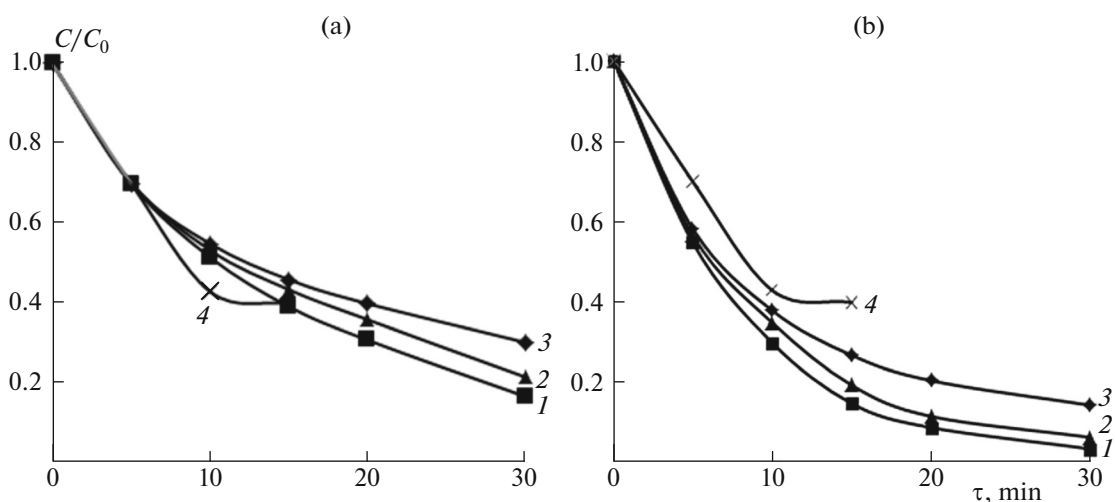


Fig. 4. Results of investigations of the PCA under the light action of a UV range of samples, containing 0.1 (curve 1), 0.5 (curve 2) and 1.0 mol % (curve 3) of Zn²⁺, calcined at (a) 500°C and (b) 600°C (b) and control sample Degussa P25 (curve 4).

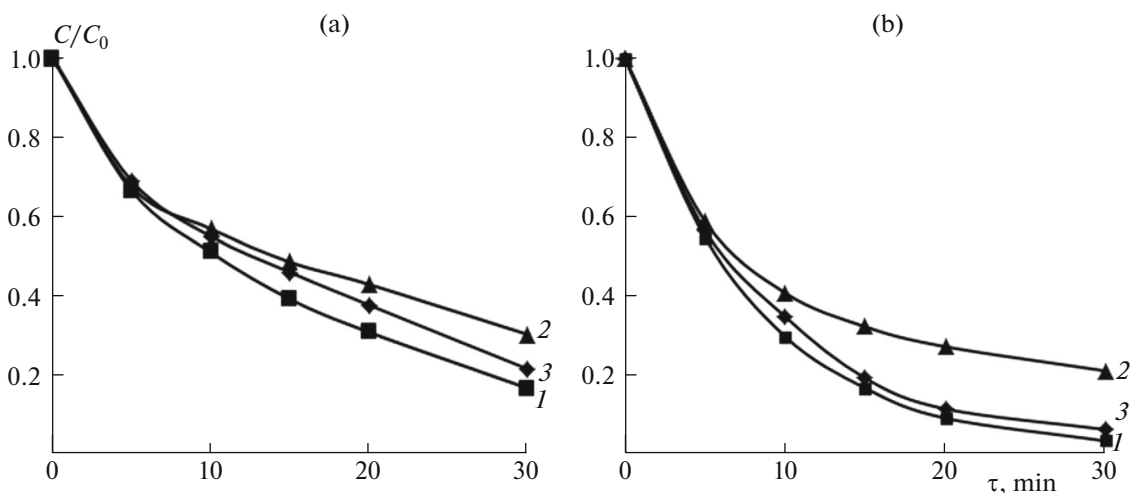


Fig. 5. Result of action of visible light on the PCA activity of nanomaterials containing 0.1 (curve 1), 0.5 (curve 2) and 1.0 mol % of Zn²⁺ (curve 3) after thermal treatment at (a) 500°C and (b) 600°C.

inert with respect to catalysis will decrease the PCA [23]. An optimum balance between these two tendencies can be found experimentally. Among the materials studied, material containing Zn²⁺ in amount of 0.1 mol % has the best photocatalytic properties under action of either UV or visible light, and this optimal composition confirms the results of [24].

CONCLUSIONS

A simple and economical method for the synthesis of materials based on titanium dioxide modified with Zn(II) in the concentration range from 0.1 to 1.0 mol % has been proposed. This method is a low-temperature synthesis of the intermediate compounds Ti(IV) and Zn(II) followed by their thermal treatment. The mate-

rials obtained are nanodisperse and one-phase, and they are crystallized in an anatase structure and thermally stable to 800°C. It was found that such materials are photocatalytically active in both UV and the visible spectral regions. The UV-radiation-induced PCA of these materials is higher than that of Degussa P25 commercial material, which is pure titanium dioxide. The highest degree of PCA was found for the material containing 0.1 mol % of Zn²⁺ and calcined at 600°C.

ACKNOWLEDGMENTS

The authors thank Current Microscopy, the center of collective use of scientific equipment at Southern Federal University, for the study of sample microstructure.

REFERENCES

1. Y. Chen, J. Y. Wang, W. Z. Li, and M. T. Ju, *J. Mater. Eng.* **44**, 103 (2016). doi 10.11868/j.issn.1001-4381.2016.03.017
2. R. Fagan, D. E. McCormack, D. D. Dionysiou, and S. C. Pillai, *Mater. Sci. Semicond. Process.* **42**, 2 (2016). doi 10.1016/j.mssp.2015.07.052
3. Z. R. Ismagilov, L. T. Tsikoza, N. V. Shikina, V. F. Zarytova, V. V. Zinoviev, and S. N. Zagrebelnyi, *Russ. Chem. Rev.* **78**, 873 (2009). doi 10.1070/RC2009v078n09ABEH004082
4. M. Pérez-González, S. A. Tomás, J. Santoyo-Salazar, and M. Morales-Luna, *Ceram. Int.* **43**, 8831 (2017). doi 10.1016/j.ceramint.2017.04.016
5. C. Wang, H. Liu, and Y. Qu, *J. Nanomater.* **2013**, 319637 (2013). doi 10.1155/2013/319637
6. C. L. Bianchi, E. Colombo, S. Gatto, et al., *J. Photochem. Photobiol., A* **280**, 27 (2014). doi 10.1016/j.jphotochem.2014.02.002
7. A. Buthiyappan, A. R. Abdul Aziz, and W. M. A. van Daud, *Rev. Chem. Eng.* **32**, 1 (2016). doi 10.1515/revce-2015-0034
8. H. Wang and C. You, *J. Chem. Eng.* **292**, 199 (2016). doi 10.1016/j.cej.2016.02.017
9. S. H. Yoon, *Appl. Surf. Sci.* **423**, 71 (2017). doi 10.1016/j.apsusc.2017.06.147
10. Y. Li, Y. Bian, Y. Zhang, and Z. Bian, *Appl. Catal., B* **206**, 293 (2017). doi 10.1016/j.apcatb.2017.01.044
11. J. Li, X. Yang, and T. Ishigaki, *J. Phys. Chem. B* **110**, 14611 (2006). doi 10.1021/jp0620421
12. L. G. Devi and R. Kavitha, *Appl. Catal. B* **140–141**, 559 (2013). doi 10.1016/j.apcatb.2013.04.035
13. V. Etacheri, C. D. Valentin, J. Schneider, et al., *J. Photochem. Photobiol., C* **25**, 1 (2015). doi 10.1016/j.jphotochemrev.2015.08.003
14. M. Pelaez, N. T. Nolan, S. C. Pillai, et al., *Appl. Catal. B: Environ.* **125**, 331 (2012). doi 10.1016/j.apcatb.2012.05.036
15. S. A. Bakar and C. Ribeiro, *J. Photochem. Photobiol., C* **27**, 1 (2016). doi 10.1016/j.jphotochemrev.2016.05.001
16. T. Umabayashi, T. Yamaki, S. Yamamoto, et al., *J. Appl. Phys.* **93**, 5156 (2003). doi 10.1063/1.1565693
17. M. Fronzi, A. Iwaszuk, A. Lucid, and M. Nolan, *J. Phys.: Condens. Matter* **28**, 23 (2016). doi 10.1088/0953-8984/28/7/074006
18. M. Hamadani, S. Karimzadeh, V. Jabbari, and D. Villagrán, *Mater. Sci. Semicond. Proc.* **41**, 168 (2016). doi 10.1016/j.mssp.2015.06.085
19. M. Anpo, *Pure Appl. Chem.* **72**, 1787 (2000). doi 10.1351/pac200072091787
20. A. Fuerte, M. D. Hernández-Alonso, A. J. Maira, et al., *Chem. Commun., No. 24*, 2718 (2001). doi 10.1039/b107314a
21. H. Yamashita, *J. Synchrotr. Radiat.* **8**, 569 (2001).
22. S. N. Phattalung, S. Limpijumnong, and J. Yu, *Appl. Catal., B* **200**, 1 (2017). doi 10.1016/j.apcatb.2016.06.054
23. L. G. Devi, B. N. Murthy, and S. G. Kumar, *Mater. Sci. Eng. B* **166**, 1 (2010). doi 10.1016/j.mseb.2009.09.008
24. C. Chen, Z. Wang, S. Ruan, et al., *Dyes Pigments* **77**, 204 (2008). doi 10.1016/j.dyepig.2007.05.003
25. Y. H. Lin, T. K. Tseng, and H. Chu, *Appl. Catal., A* **469**, 221 (2014). doi 10.1016/j.apcata.2013.10.006
26. S. Chen, W. Zhao, W. Liu, and S. Zhang, *Appl. Surf. Sci.* **255**, 2478 (2008).
27. J. N. Deng, B. Yu, and Z. Lou, *Sens. Actuators, B* **184**, 21 (2013).
28. Y. Ku, Y. H. Huang, and Y. C. Chou, *J. Mol. Catal., A* **342–343**, 18 (2011). doi 10.1016/j.molcata.2011.04.003
29. G. K. Prasad, P.V.R.K. Ramacharyulu, B. Singh, et al., *J. Mol. Catal., A* **349**, 55 (2011). doi 10.1016/j.molcata.2011.08.018
30. E. M. Bayan, T. G. Lupeiko, L. E. Pustovaya, and A. G. Fedorenko, *Springer Proc. Phys.* **175**, 51 (2016). doi 10.1007/978-3-319-26324-3_4
31. E. M. Bayan, T. G. Lupeiko, L. E. Pustovaya, and A. G. Fedorenko, *Nanotechnol. Russ.* **12**, 269 (2017). doi 10.1134/S199507801703003X
32. E. M. Bayan, T. G. Lupeiko, E. V. Kolupaeva, et al., *Springer Proc. Phys.* **193**, 17 (2017). doi 10.1007/978-3-319-56062-5_2
33. V. Stengl, S. Bakardjieva, and N. Murafa, *Mater. Chem. Phys.* **114**, 217 (2009). doi 10.1016/j.matchemphys.2008.09.025
34. L. Wang, X. Fu, Y. Han, et al., *J. Nanomater.* **2013**, 321459 (2013). doi 10.1155/2013/321459
35. E. M. Bayan, T. G. Lupeiko, L. E. Pustovaya, A. A. Knyashchuk and A. G. Fedorenko, *Russ. J. Phys. Chem. B* **11**, 600 (2017). doi 10.1134/S1990793117040042
36. S. Silvestr and E. L. Foletto, *Ceram. Int.* **43**, 14057 (2017). doi 10.1016/j.ceramint.2017.07.140
37. B. Palanisamy, C. M. Babu, B. Sundaravel, et al., *J. Hazard. Mater.* **252**, 233 (2013). doi 10.1016/j.jhazmat.2013.02.060
38. M. Crisan, N. Dragan, D. Crisan, et al., *Ceram. Int.* **42**, 3088 (2016). doi 10.1016/j.ceramint.2015.10.097
39. N. Khatun, P. Rajput, D. Bhattacharya, et al., *Ceram. Int.* **43**, 14128 (2017). doi 10.1016/j.ceramint.2017.07.153
40. Y. Jiang, Y. Sun, H. Liu, et al., *Dyes Pigments* **78**, 77 (2008). doi 10.1016/j.dyepig.2007.10.009
41. Z. Liu, C. Liu, J. Ya, and E. Lei, *Renew. Energy* **36**, 1177 (2011). doi 10.1016/j.renene.2010.09.019

Translated by S. Lebedev